LeuT Conformational Sampling Utilizing Accelerated Molecular Dynamics and Principal Component Analysis

James R. Thomas,[†] Patrick C. Gedeon,[†§] Barry J. Grant,[‡] and Jeffry D. Madura[†*]
[†]Department of Chemistry and Biochemistry and the Center for Computational Sciences, Duquesne University, Pittsburgh, Pennsylvania; [‡]Center for Computational Medicine and Bioinformatics, University of Michigan, Ann Arbor, Michigan; and [§]School of Medicine, Temple University, Philadelphia, Pennsylvania

ABSTRACT Monoamine transporters (MATs) function by coupling ion gradients to the transport of dopamine, norepinephrine, or serotonin. Despite their importance in regulating neurotransmission, the exact conformational mechanism by which MATs function remains elusive. To this end, we have performed seven 250 ns accelerated molecular dynamics simulations of the leucine transporter, a model for neurotransmitter MATs. By varying the presence of binding-pocket leucine substrate and sodium ions, we have sampled plausible conformational states representative of the substrate transport cycle. The resulting trajectories were analyzed using principal component analysis of transmembrane helices 1b and 6a. This analysis revealed seven unique structures: two of the obtained conformations are similar to the currently published crystallographic structures, one conformation is similar to a proposed open inward structure, and four conformations represent novel structures of potential importance to the transport cycle. Further analysis reveals that the presence of binding-pocket sodium ions is necessary to stabilize the locked-occluded and open-inward conformations.

Received for publication 28 November 2011 and in final form 3 May 2012.

*Correspondence: madura@duq.edu

Monoamine transporters (MATs) belong to a group of homologous transmembrane proteins that function by Na^+/Cl^--dependent secondary active transport. The transmembrane location of the transporters at synaptic terminals allows for the reuptake of neurotransmitters and, consequentially, termination of signaling in the chemical synapse (1). Dysregulation of MATs and the resultant imbalance of their substrates—dopamine, serotonin, or norepinephrine—has long been implicated in conditions such as major depression, Parkinson's disease, and addiction (1–3). Furthermore, MATs are the target of a wide variety of pharmacological compounds such as selective serotonin reuptake inhibitors (4). The three-dimensional structure of these transporters and the conformational mechanism by which they function remain unknown.

In 2005, the crystallographic structure of the bacterial Na^+-dependent leucine transporter (LeuT), a close homolog of the eukaryote MATs (5), was solved. Since then, the crystallographic LeuT structure has been used as a template to model eukaryote MATs in three dimensions (6–9). By examining the LeuT directly, it is possible to avoid introducing any uncertainty into the homology modeling process.

Although they have offered some insight into the dynamics of the substrate binding pocket, previous computational efforts utilizing MD to determine the substrate transport mechanism of LeuT and MAT homology models have fallen short of the goal of elucidating the full substrate transport mechanism. This is most likely due to limitations in computational power, as the longest simulations to date run on the order of a few microseconds and use standard or steered molecular dynamics (9–14), a computational algorithm that is probably insufficient to overcome energy barriers and allow conformational transitions to novel states.

As a solution to this problem, we begin with a previously reported equilibrated structure (11), implement the use of an accelerated molecular dynamics (aMD) algorithm (15), and conduct seven 250-ns aMD simulations. The advantage of using aMD for conformational sampling is that the algorithm adds an energy bias factor when the total energy of a system falls below a predetermined threshold, preventing the slowing or practical lockdown of a system if it falls into a particularly deep energy well. However, the bias factor still allows the simulation to stay in a particular minimum long enough to allow individual minima to be defined (15).

To observe different conformational states, we applied the aMD simulation protocol to seven different starting scenarios, beginning with the LeuT protein and POPE membrane from a 30-ns equilibrated system published previously (11). The seven different simulation setups were created by varying the presence of binding-pocket leucine substrate and sodium ions (Table 1). Using tools within AMBER 9 (16), each system was solvated using TIP3 water, and sodium and chloride ions were added. The resulting systems were energy-minimized to slowly heat the systems to 310 K. At 310 K, MD calculations were performed for 5 ns. The aMD simulation protocol was then carried out over 250 ns for each of the simulation setups (Table 1).

We then analyzed the aMD trajectories using principal component analysis (PCA). PCA allows for the calculation of variations between data sets across several dimensions and generates a set of vectors representing the greatest

Editor: Nathan Baker.

doi: 10.1016/j.bpj.2012.05.002

TABLE 1 Combinations of leucine, sodium, and substrates in each simulation

Simulation	Color	Leu	Na1	Na2
1	Red	+	+	+
2	Orange	+	+	−
3	Yellow	−	+	+
4	Green	−	−	+
5	Blue	−	+	−
6	Light blue	+	−	+
7	Purple	−	−	−

Color indicates the color of the simulation in Fig. 1. Labeling of the sodium binding pockets follows the Gouaux model (5,20).

variance (17,18). When the vectors of the largest variance are plotted against each other, similar structures cluster together, whereas more diverse structures are separated by a distance.

In a complementary analysis, PCA was performed on the C_α positions of previously published LeuT structures to determine which individual transmembrane domains or combinations of domains yielded the greatest and most distinct separation of values. The published structures utilized were the 20 LeuT crystal structures available in the Research Collaboratory for Structural Bioinformatics (RCSB) Protein Data Bank (5,12,19–23) and two proposed open-inward conformations (24). This PCA calculation was performed using both the ptraj package in AMBER9 (16) and the Bio3D package for R (25). The greatest discrimination between these structures was evident when the combination of transmembrane helical domains (TMs) 1b and 6a, also proposed to be involved in transport (9,21,26), was used for the analysis. The method of performing PCA on only specific sections of a protein for a focused analysis has previously been reported (27).

PCA was performed for each simulation trajectory using the TM1b/6a combination. Structures were isolated from the simulation every 200 ps and superimposed so that statistical analysis would be carried out on an average structure.

The graph of the PCA for all simulations revealed seven clusters. A representative structure was removed from the densest section of each cluster and minimized, as were the two proposed inward conformations. The PCA graph with the minimized structures is shown in Fig. 1, and the root mean-squared deviation (RMSD) values between the structures are shown in Table S1 in the Supporting Material. All structures had starting points around the 2A65 occluded structure. The two simulations with both sodium ions bound but differing in the presence of leucine substrate (Table 1, simulations 1 and 3) mostly remained in the occluded conformation, with a few sparse points where they sampled a structure from another cluster. The relative stability of the leucine-bound structure has been seen experimentally by the decreased transport rate compared to the alanine-bound structure (28). It has been proposed that leucine may not be the proper or natural substrate because its extremely high affinity for LeuT may stabilize the occluded structure (29). The structure without leucine (simulation 3) appeared to have similar sampling, as it is stabilized by both sodium ions,

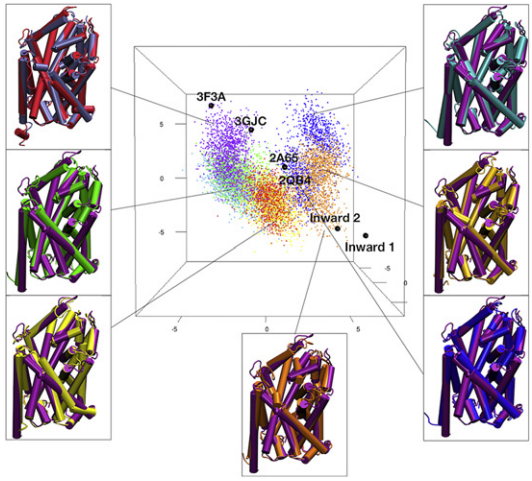

FIGURE 1 Scatter plot of the PCA for all simulations colored according to Table 1. Select crystal structures and the modeled inward structures (24) are displayed as black spheres. Simulation structures corresponding to a clustered group are shown superimposed upon the 2A65 structure in purple or the 3F3A structure shown in red for the topmost left cluster. See Fig. S3 in the Supporting Material for a larger representation.

although there was a small amount of sampling from other clusters that did not occur with the leucine substrate present.

Analysis of the presence and absence of binding-pocket sodium in Na1 has yielded interesting results. All clusters on the left are without an occupied Na1 site, whereas all clusters on the right of the graph have Na1 occupied. Analysis reveals that the occupancy of Na1 and the leucine substrate in the absence of Na2 generates a conformation similar to the inward conformation proposed by Tajkhorshid et al. (24). The original proposal contained two inward-facing structures modeled by steering the backbone of LeuT toward the crystallized open-inward conformation of the related protein vSGLT (24). Here, using a different approach, the aMD analysis corroborates the potential validity of this conformation, as throughout the course of aMD simulation, the TM 1b and 6a regions took on a conformation similar to that in the proposed open-inward conformation. Similarly, the simulation with only Na1 occupied (simulation 5) appears close to the inward conformations. Our conformation suggests that since, as proposed, intracellular solvent accessibility to Na2 destabilizes the occluded conformation and facilitates transport, but the selectivity of the Na1 binding site for sodium ions is governed by the presence of sodium in Na2, then the Na1 site has an expanded role and facilitates or stabilizes the transition to an inward conformation (13,14).

The simulation with apo-LeuT started at the occluded structure and eventually sampled a conformation similar to the LeuT inhibited with Trp in an open-outward conformation (RCSB ID 3F3A) (21). Preliminary analysis reveals that the sampled open-outward structure and 3F3A have an RMSD of 1.3 Å for the C_α positions of the core TM domains (TMs 1–10).

It should be noted that although no transport of either sodium or leucine occurred in any simulation, the application of aMD and PCA upon the LeuT structure has proven an effective combination—especially when compared to the crystallized apo-LeuT structure released during the review of this article (30). A more detailed analysis of this structure compared to the simulation data is found in the Supporting Material. The three primary points of the alternating-access mechanism—open-outward, occluded, and open-inward—appear to have been simulated using only an occluded structure as a starting point. In addition, four unique structures have been identified and are believed to represent other steps involved in the transport cycle. Further investigation of these structures, including analysis of specific residues and their proposed involvement in the transport mechanism, will be released in a future publication.

SUPPORTING MATERIAL

Supplementary methods, results, acknowledgments of developments during revisions, eight figures, three tables, and references (31,32) are available at http://www.biophysj.org/biophysj/supplemental/S0006-3495(12)00554-1.

ACKNOWLEDGMENTS

We thank Donald Hamelberg for supplying both assistance and the code for aMD and Cesar Oliveira for help with reweighting the PCA results.

This work was supported by the National Institutes of Health, National Science Foundation, Department of Defense, and the U.S. Department of Education under awards 5R01DA27806-2, CHE-1005145(REU/ASSURE), CHE-0723109(MRI), and P116Z080180.

REFERENCES and FOOTNOTES

1. Surratt, C. K., O. T. Ukairo, and S. Ramanujapuram. 2005. Recognition of psychostimulants, antidepressants, and other inhibitors of synaptic neurotransmitter uptake by the plasma membrane monoamine transporters. *AAPS J.* 7:E739–E751.
2. Ritz, M. C., R. J. Lamb, …, M. J. Kuhar. 1987. Cocaine receptors on dopamine transporters are related to self-administration of cocaine. *Science.* 237:1219–1223.
3. Haapaniemi, T. H., A. Ahonen, …, V. V. Myllylä. 2001. 123Iβ-CIT SPECT demonstrates decreased brain dopamine and serotonin transporter levels in untreated parkinsonian patients. *Mov. Disord.* 16:124–130.
4. Meyer, J. H., A. A. Wilson, …, S. Houle. 2001. Occupancy of serotonin transporters by paroxetine and citalopram during treatment of depression: a [(11)C]DASB PET imaging study. *Am. J. Psychiatry.* 158:1843–1849.
5. Yamashita, A., S. K. Singh, …, E. Gouaux. 2005. Crystal structure of a bacterial homologue of Na^+/Cl^--dependent neurotransmitter transporters. *Nature.* 437:215–223.
6. Indarte, M., J. D. Madura, and C. K. Surratt. 2006. Comparative Molecular Modeling of the Dopamine Transporter Using the Leucine Transporter LeuTaA as a Template. Society For Neuroscience, Atlanta, GA.
7. Indarte, M., J. D. Madura, and C. K. Surratt. 2008. Dopamine transporter comparative molecular modeling and binding site prediction using the LeuT(Aa) leucine transporter as a template. *Proteins.* 70:1033–1046.
8. Beuming, T., L. Shi, …, H. Weinstein. 2006. A comprehensive structure-based alignment of prokaryotic and eukaryotic neurotransmitter/Na^+ symporters (NSS) aids in the use of the LeuT structure to probe NSS structure and function. *Mol. Pharmacol.* 70:1630–1642.
9. Shan, J., J. A. Javitch, …, H. Weinstein. 2011. The substrate-driven transition to an inward-facing conformation in the functional mechanism of the dopamine transporter. *PLoS ONE.* 6:e16350.
10. Zhao, Y., D. Terry, …, J. A. Javitch. 2010. Single-molecule dynamics of gating in a neurotransmitter transporter homologue. *Nature.* 465:188–193.
11. Gedeon, P. C., M. Indarte, …, J. D. Madura. 2010. Molecular dynamics of leucine and dopamine transporter proteins in a model cell membrane lipid bilayer. *Proteins.* 78:797–811.
12. Quick, M., A.-M. L. Winther, …, J. A. Javitch. 2009. Binding of an octylglucoside detergent molecule in the second substrate (S2) site of LeuT establishes an inhibitor-bound conformation. *Proc. Natl. Acad. Sci. USA.* 106:5563–5568.
13. Noskov, S. Y., and B. Roux. 2008. Control of ion selectivity in LeuT: two Na^+ binding sites with two different mechanisms. *J. Mol. Biol.* 377:804–818.
14. Zhao, C., and S. Y. Noskov. 2011. The role of local hydration and hydrogen-bonding dynamics in ion and solute release from ion-coupled secondary transporters. *Biochemistry.* 50:1848–1856.
15. Hamelberg, D., J. Mongan, and J. A. McCammon. 2004. Accelerated molecular dynamics: a promising and efficient simulation method for biomolecules. *J. Chem. Phys.* 120:11919–11929.
16. Case, D. A., T. A. Darden, …, P. A. Kollman. 2006. AMBER 9. University of California, San Francisco, CA.
17. Maisuradze, G. G., A. Liwo, and H. A. Scheraga. 2009. Principal component analysis for protein folding dynamics. *J. Mol. Biol.* 385:312–329.
18. Stein, S., A. Loccisano, …, J. Evanseck. 2006. Principal components analysis: a review of its application on molecular dynamics data. *Annu. Rep. Comput. Chem.* 2:233–261.
19. Zhou, Z., J. Zhen, …, D. N. Wang. 2007. LeuT-desipramine structure reveals how antidepressants block neurotransmitter reuptake. *Science.* 317:1390–1393.
20. Singh, S. K., A. Yamashita, and E. Gouaux. 2007. Antidepressant binding site in a bacterial homologue of neurotransmitter transporters. *Nature.* 448:952–956.
21. Singh, S. K., C. L. Piscitelli, …, E. Gouaux. 2008. A competitive inhibitor traps LeuT in an open-to-out conformation. *Science.* 322:1655–1661.
22. Zhou, Z., J. Zhen, …, D. N. Wang. 2009. Antidepressant specificity of serotonin transporter suggested by three LeuT-SSRI structures. *Nat. Struct. Mol. Biol.* 16:652–657.
23. Kroncke, B. M., P. S. Horanyi, and L. Columbus. 2010. Structural origins of nitroxide side chain dynamics on membrane protein α-helical sites. *Biochemistry.* 49:10045–10060.
24. Shaikh, S. A., and E. Tajkhorshid. 2010. Modeling and dynamics of the inward-facing state of a Na^+/Cl^- dependent neurotransmitter transporter homologue. *PLoS Comput. Biol.* 6:6.
25. Grant, B. J., A. P. C. Rodrigues, …, L. S. Caves. 2006. Bio3d: an R package for the comparative analysis of protein structures. *Bioinformatics.* 22:2695–2696.
26. Forrest, L. R., and G. Rudnick. 2009. The rocking bundle: a mechanism for ion-coupled solute flux by symmetrical transporters. *Physiology (Bethesda).* 24:377–386.
27. Schulze, B. G., and J. D. Evanseck. 1999. Cooperative role of Arg^{45} and His^{64} in the spectroscopic A 3 state of carbonmonoxy myoglobin: molecular dynamics simulations, multivariate analysis, and quantum mechanical computations. *J. Am. Chem. Soc.* 121:6444–6454.
28. Shi, L., M. Quick, …, J. A. Javitch. 2008. The mechanism of a neurotransmitter:sodium symporter—inward release of Na^+ and substrate is triggered by substrate in a second binding site. *Mol. Cell.* 30:667–677.
29. Zhao, Y., D. S. Terry, …, J. A. Javitch. 2011. Substrate-modulated gating dynamics in a Na^+-coupled neurotransmitter transporter homologue. *Nature.* 474:109–113.
30. Krishnamurthy, H., and E. Gouaux. 2012. X-ray structures of LeuT in substrate-free outward-open and apo inward-open states. *Nature.* 481:469–474.
31. R: A Language and Environment for Statistical Computing. R Foundation for Statistical Computing, Vienna, Austria.
32. MOE: Molecular Operating Environment. Chemical Computing Group, Montreal, Quebec, Canada.